

ICCHMT 2018, Cracow, Poland, 21-24 May 2018

“Put the paper number here”XXX

## ENERGY TRANSFER INCLUDING SOLID-LIQUID PHASE TRANSFORMATION ASPECTS IN MODELLING OF ADDITIVE LAYER MANUFACTURING USING LATTICE BOLTZMANN – CELLULAR AUTOMATA METHODS

Dmytro Svyetlichnyy<sup>1\*</sup> and Michal Krzyzanowski<sup>1,2</sup><sup>1</sup>Faculty of Metals Engineering and Industrial Computer Science,  
AGH University of Science and Technology, Al. Mickiewicza 30, 30-059 Krakow, Poland<sup>2</sup>Faculty of Computing, Engineering and The Built Environment,  
Birmingham City University, Birmingham, UK\*Correspondence author: Email: [svetlich@metal.agh.edu.pl](mailto:svetlich@metal.agh.edu.pl)

Keywords: Additive manufacturing, Selective laser sintering/melting, Modelling, Lattice Boltzmann method, Cellular automata, Heat transfer, Phase transformation.

### ABSTRACT

The detailed analysis of energy transfer including solid-liquid phase transformation during laser assisted additive layer manufacturing (ALM) process is presented as part of currently developing holistic numerical model based on Lattice Boltzmann and cellular automata methods (LBM-CA). The presented results are mainly related to consideration of melting and solidification of the powder bed including of the free surface flow, wettability, surface tension and other relevant phenomena showing good agreement with available experimental results and theoretical predictions.

### NOMENCLATURE

$b_T$	- the discrete velocity at the temperature $T$ ;
$e$	- the phase space variable;
$f(\mathbf{x}, \mathbf{v}, t)$	- the particles distribution function;
$f_i^{eq}$	- the equilibrium distribution function of $i^{\text{th}}$ discrete velocity;
$\mathbf{F}$	- the external force (e.g., gravity);
$g_i$	- the distribution function for the thermal (diffusion-convection) problem;
$g_i^{eq}$	- the equilibrium distribution function for the thermal (diffusion-convection) problem;
$m$	- mass;
$S$	- the heat source;
$t$	- the time;
$\mathbf{x}$	- the phase space variable;

$\mathbf{v}$	- a vector of the macroscopic velocity;
$\tau$	- the relaxation time;
$\tau_T$	- the relaxation time at the temperature $T$ ;
$\rho$	- the macroscopic density;

### INTRODUCTION

A new holistic numerical model based on Lattice Boltzmann and cellular automata methods (LBM-CA) is currently under development within a frame of an integrated modelling approach applied for studying the complex relationship between different physical mechanisms taking place during laser assisted additive layer manufacturing (ALM) [1]. The entire ALM process has been analysed and divided on several stages considering a powder bed deposition, laser energy absorption and heating of the powder bed by the moving highly concentrated energy source leading to powder melting, fluid flow in the melted pool and through partly or not melted material, and solidification. The presented earlier results included the entire structure of the model consisting of different modules connected together demonstrating the homogeneity of the proposed holistic model. The modules, considering the mentioned above physical phenomena, were developed to different extent leaving many aspects of this integrated numerical approach for further consideration and analysis.

The aim of this work is more detailed analysis of energy transfer including solid-liquid phase transformation during the ALM process. The

presented results are mainly related to consideration of melting and solidification of the powder bed including of the free surface flow, wettability, surface tension and other relevant phenomena.

## ANALYSIS AND MODELLING

Initially, the absorbed thermal energy spreads by heat diffusion [2, 3]. The solid-liquid phase transformation starts when the temperature in the affected zone exceeds the solidus temperature. After consuming latent heat, when the volume of liquid phase exceeds a threshold, the solid particulate material exhibit signs of liquid behaviour, where heat transport is described by diffusion or convection including radiation and convection heat transfer from the liquid surface. The excess heat in the area of the liquid phase is dissipated by heat conduction into the deeper layers of the powder bed leading to re-solidification of the melt pool. The different stages and fragments of LBM-CA model development are presented and discussed.

In selective laser sintering/melting (SLS/SLM) technology, a moving laser beam melts selectively the deposited metal and/or metal composite powder materials into a three-dimensional part of the final product [4]. The product is manufactured in the chamber located on a movable platform that adjusts its height equal to the thickness of the forming layer. Powder is added from the powder feed device and levelled with a roller or using other methods. Powder is deposited on the top of the powder bed in the build chamber, which contains the previously melted and solidified layer of the product and an unprocessed amount of powder. Then, a new layer is melted with the laser beam and the cycles are repeated until the final product is obtained.

The mentioned technological operations cannot always be exactly reflected by the corresponding mathematical models (Fig.1). The physically based models should be developed considering the key physical processes and phenomena taking place in the material. Thus, the following five main processes or phenomena have been considered for the modelling:

- powder bed generation (PBG);
- laser beam heat treatment (LBH);
- melting (M);
- free flow of melted material (LF);
- solidification (S).

The mentioned processes and phenomena take place sequentially or simultaneously. The corresponding individual mathematical models can be quite sophisticated themselves requiring more details from each of those processes. As a first approach, they can be simulated using the following four models:

1. Powder bed generation model (PBG);
2. Heat exchange and transfer model (HE&T);
3. Thermal solid-liquid interface (SLIT);
4. Mechanical solid-liquid interface (SLIM).

However sometimes, it's easier to perform the relevant calculations when the state of matter is explicitly defined by an appropriate variable. Then, the state variable should be attached to every cell. The following three states of matter are considered in the model: solid, liquid and gas. However, a cell can contain different materials or can contain the same material but in the different state of matter. Taking this into consideration, four values of the state variable are added for description of the cells containing material(s) in different states of matter. Thus, the following values of the state variable are assumed for each cell in further consideration indicating the state of the cell:

G – gas, the whole cell is filled with gas;

L – liquid;

S – solid (obstacle);

LG – liquid-gas interface, the cell is partially filled with gas, the remaining is filled with liquid;

SG – the cell filled with gas located near the obstacle;

LG – the cell filled with liquid near the obstacle;

SLG – liquid-gas interface near the obstacle.

State diagram is presented in Fig.2. The cells containing gas are presented as white, or they have a white segment. Correspondingly, the cells containing liquid are presented as blue while those containing solid material are highlighted as grey.

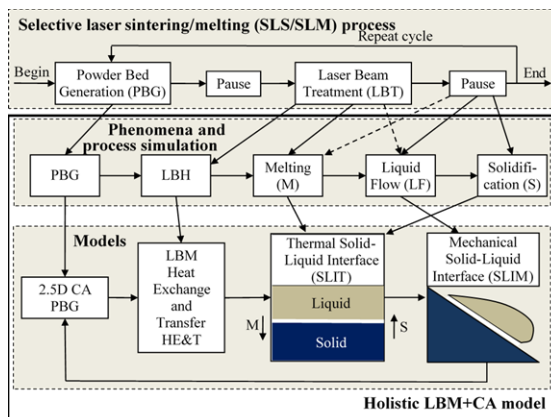


Figure 1

Block diagram of SLS/SLM process, modelling phenomena and main models for simulation.

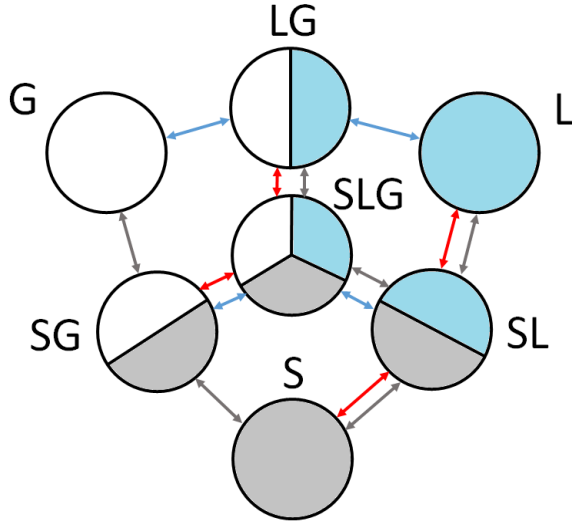


Figure 2  
The state diagram

Three kinds of state changes are considered in the presented state diagram. They are marked by arrows of different colors. The blue arrows represent a hydrodynamic component, i.e. liquid flow with free surface. There are two following transitions here: L-LG-G and SL-SLG-SG. The first transition represents movement of the liquid under the surface tension, gravity and inertia. The second one, in addition, takes into account a wettability. This part of the state diagram is considered in the model completely. The second kind of transition is shown in the state diagram by red arrows. They represent phase transition, in other words, changes of the state of matter. At this stage, the only transition assumed in the model was solid-liquid transition with presence of gas phase, such as SG-SLG-LG; and without gas phase, S-SL-L. The third kind of transitions presented in the state diagram is connected with movement of solid phase. It is represented by grey arrows.

The whole holistic model is developed on the basis of the LBM with elements of CA [5,6]. The LBM is a discrete numerical method for solution of the Boltzmann transport equation:

$$\frac{\partial f}{\partial t} + \frac{\partial f}{\partial \mathbf{x}} \cdot \mathbf{e} + \frac{\mathbf{F}}{m} \cdot \frac{\partial f}{\partial \mathbf{e}} = \Omega \quad (1)$$

Particle velocity space can be reduced to a set of discrete velocities  $\{\mathbf{e}_i, i = 1, \dots, b\}$  and the construction of the lattice, on which the calculations are carried out. Normally, the equation is approximated along characteristic velocity vectors using trapezoidal rule in space and explicit Euler scheme for the time derivative:

$$f_i(\mathbf{x} + \mathbf{e}_i, t + 1) = f_i(\mathbf{x}, t) - \frac{1}{\tau} [f_i(\mathbf{x}, t) - f_i^{eq}(\mathbf{x}, t)] + F_i \quad (2)$$

Eq. (2) is solved numerically in two consecutive stages, namely: streaming and collision.

The macroscopic density  $\rho$  and momentum  $\rho \mathbf{v}$  in a cell are the 0<sup>th</sup> and 1<sup>st</sup> moments of the distribution functions:

$$\rho = \sum_{i=0}^b f_i, \quad \rho \mathbf{v} = \sum_{i=0}^b f_i \mathbf{e}_i \quad (3)$$

The distribution function  $g_i$  for the thermal (diffusion-convection) problem is expressed in the following form:

$$g_i(\mathbf{x} + \mathbf{e}_i, t) = g_i(\mathbf{x}, t) - \frac{1}{\tau_T} [g_i(\mathbf{x}, t) - g_i^{eq}(\mathbf{x}, t)] + \frac{1}{b_T} S \quad (4)$$

The temperature  $T$  is expressed as the following sum:

$$T = \sum_{i=0}^{b_T} g_i \quad (5)$$

For both hydrodynamic and thermal tasks the same velocity model D2Q9 is applied  $b = b_T = 8$ .

## RESULTS AND DISCUSSION

The main results of the consequent stages related to the model development are shown in this section.

**Liquid flow with free surface:** Change of the shape of a drop of liquid from rectangular to round under the effect of surface tension is shown in Fig.3.



Figure 3  
Modelling results illustrating influence of the surface tension on the shape of a drop of liquid

Fig.4 illustrates the surface shape in consideration of surface tension, gravity and wettability showing the drops of liquid on horizontal surface and liquid in the vessel with vertical walls. Wettability is related to the attempt of a solid to form a common interface with a liquid and can be measured by the contact angle  $\alpha$ . The corresponding values of  $\cos \alpha$  presented in Fig.4 are equal to -0.5; 0 and 0.5.

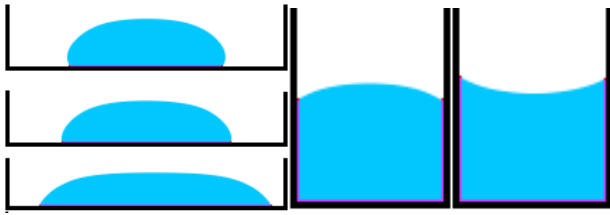


Figure 4

Modelling results illustrating influence of wettability on the shape of liquid surface

Fig. 5 illustrates next stages of the simulation, such as liquid flow along a more complex pattern compared with obstacle free flow. The examples of such modelling are presented in Fig.5.

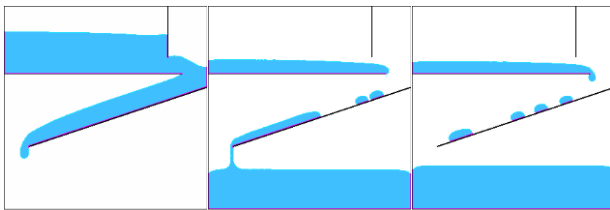


Figure 5

Simulation of liquid flow

**Phase transition:** The next stage is investigation of the applicability of the developed model based on LBM for thermal applications. With this aim, a solid-liquid interface was implemented into the modelling. The interface allows for simulation of the phase transition and changes of the state of matter with consideration of the enthalpy of transition resulting from providing heat to a substance to change its state of matter. The thermal model is connected with the previously developed hydrodynamic model. It means that the liquid phase model takes into consideration surface tension, gravity, and wettability during the simulation. Additionally, hydrodynamic part of the model includes into consideration convection influenced by the difference of the temperature in the different areas of the liquid. Two cases of melting samples, simulated assuming convection, are presented in Fig.6a and 6b. Each case is represented by the set of four images from top left to bottom right of each set. The first image presents the temperature distribution with white and black isotherms, the black one indicates the transition temperature. The temperature distribution within liquid is presented using warm colors while the temperature of the solid phase is shown using light blue color. The second picture illustrates velocity distribution within the liquid phase, while the third and fourth pictures present

horizontal and vertical components of the velocity. The temperature of the left wall of the sample is constant and is maintained above the transition temperature, while the right wall has a temperature below the transition temperature. The results related to modelling of the first melting sample were obtained for the case when no heat transfer between the liquid and gas phases was assumed (Fig.6a). In the second case, the heat transfer was taken into account. Fig.6 clearly illustrates the effect of convection on the boundary shape between liquid and solid phases, and also the influence of boundary conditions on the simulation results.

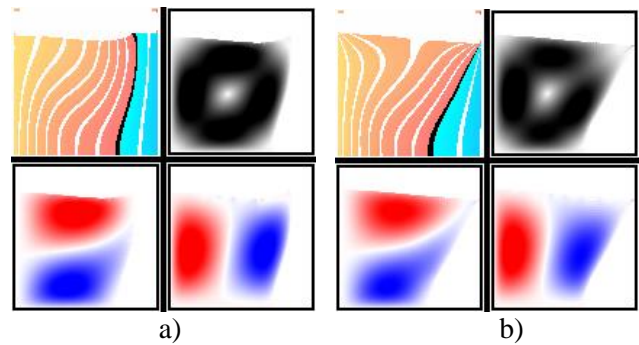


Figure 6

Modelling results illustrating melting samples simulated assuming convection

Other results of the numerical modelling based on application of LBM-CA are presented beneath. In Fig.7, a material in solid state is heated by hot gas with temperature above its melting temperature. Then, the molten material flows down collecting in the small drops. The drops gradually grow and come off the surface reaching a critical size. Then, they fall down on the bottom surface. The presented in Fig. 7 simulation results are different depending on the temperature of the bottom surface. The results illustrate the two following cases when the bottom surface temperature is above (Fig.7a) and below (Fig.7b) the transition temperature.

In spite of the relatively low temperature of the bottom surface corresponding to the second case, not the whole liquid material is solidified after dropping down on the surface, as it is shown in Fig.7b, because of higher gas temperature.

**Laser heating:** In SLS/SLM process, a laser beam scans on the top of the powder bed as a source of heat causing powder bed radiation, light absorbing, scattering, dispersion and diffraction of light in a media. The interaction between powder bed and laser

beam is very complicated and its understanding is key to description of laser energy penetration and powder bed absorption.

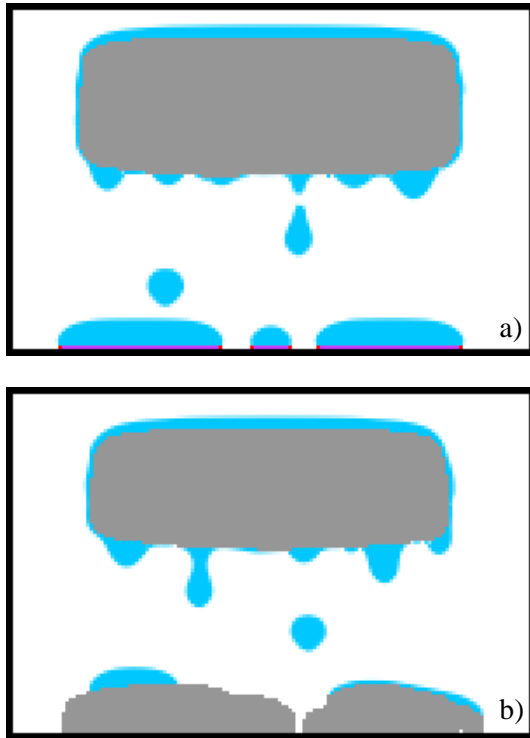


Figure 7  
Modelling results illustrating melting material falling down on the surface followed by (a) and without subsequent solidification (b)

The model of light propagation applied in this work combines elements of LBM and CA. The algorithm similar to particle tracing methods for visualization and computer graphics is used in the modelling approach. It is assumed that the laser radiation transmits light energy in gas as straight beam without scattering. Striking the surface of the liquid or solid phase, the energy is divided on the three following parts: reflected, absorbed and transmitted. If the material is opaque, the beam is not transmitted and the radiation is reflected and absorbed. The reflected energy is not considered further in the present version of the model. The light energy penetrating the material is subjected to scattering and absorption. Transmission and absorption depend on variety of the chemical and physical characteristics of the powder bed material and also on the wavelength of the incident radiation. In the model, the laser energy entering the cell is divided on the following parts. The absorbed part of the energy is transferred into heat and later used in the holistic model as a heat source  $S$  (4). The second part is considered as

an output energy, which is defined by a transferred distribution function, which describes a fraction of output light energy depending on the angle between directions of entering and exiting beams. It is assumed in the model that the material can be opaque, translucent or transparent. For instance, gas is assumed as transparent, metals are opaque and bio-active glasses are translucent materials. The coefficient of material transparency depends on both the state of matter and the temperature of bio-active glass, from low values for cold solid to high values related to hot molten bio-active glass. Some of the simulation results are presented in Fig.8-10, where the intensity of light, or the power of the light transferred per unit area, is presented by the intensity of green color. The heat source, as an absorbed part of the light energy, is shown by pink-red color. The solid material is shown in the figures as the grey area while the liquid one is presented as the blue one. In the first two results of the simulation, the point source of light energy is applied and shown in Fig.8 and 9 as a red point. While in Fig.10, the source of light energy is a laser beam striking and penetrating material.

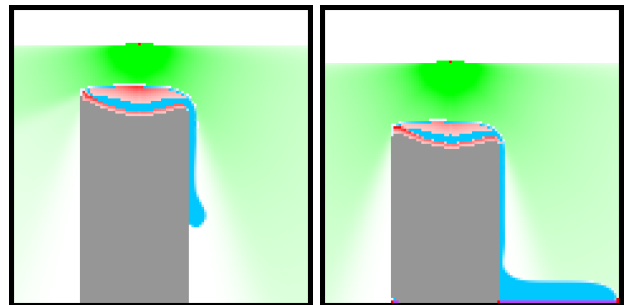


Figure 8  
Simulation results of melting solid by the light energy

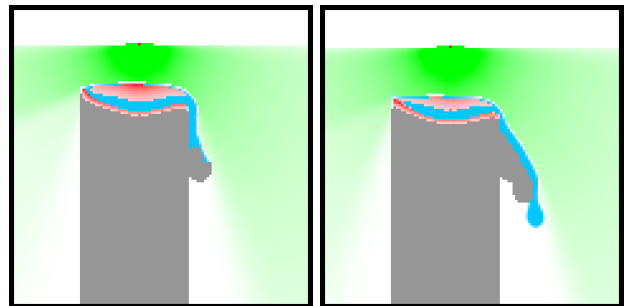


Figure 9  
Simulation results of melting solid by the light energy followed by flow and solidification



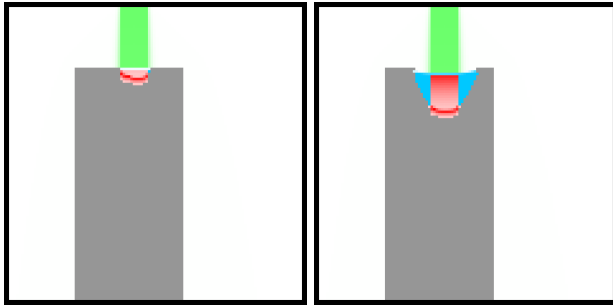


Figure 10

Simulation results of melting solid by the laser beam

In the first simulation (Fig.8), the material is melted and is flowing down as the assumed temperature conditions do not allow for solidification. The second example differs from the first one by the temperature conditions, which allowed for the material solidification in this case (Fig.9). The last simulation result presented in Fig.10 illustrates melting solid by the laser beam. The two following areas of more intensive heat absorption can be observed. The first area is located near the liquid surface, where the maximum energy flux density is observed despite high transparency of the molten material. The second area is located near the phase transition boundary, which is accompanied with the fast decrease in material transparency.

**Further model development:** The model of powder bed generation has been presented in the earlier publication [7]. At present, the developed PBG model is being combined with the models discussed in this work and the first simulation of the whole SLM process will be presented at ICCHMT 2018 followed by an extended journal publication.

## CONCLUSIONS

A numerical model based on LBM and CA methodology is currently under development. At this stage, the model includes four modules, such as powder bed generation, heat exchange and transfer, thermal solid-liquid and mechanical solid-liquid interface modules combined together within a frame of an integrated modelling approach applied with the aim of better understanding the complex relationships between different physical mechanisms occurring during multi-material laser assisted ALM. Some aspects of the obtained modelling results have been validated showing good agreement with available experimental results and theoretical predictions. Although, more work should be done, including both

modelling and experimental trials, to achieve reliable predictability of the model, the current state of the development shows a great potential of the numerical approach in terms of becoming a trustworthiness attribute of the new technology.

## ACKNOWLEDGMENTS

The support of Polish Ministry of Science and Higher Education under grant 11.11.110.498 is greatly appreciated.

## REFERENCES

1. Svyetlichyy, D., Krzyzanowski, M., Straka, R., Lach, L. and Rainforth, M., 2018, Application of Cellular Automata and Lattice Boltzmann Methods for Modelling of Additive Layer Manufacturing, *Int. J. Numerical Methods for Heat and Fluid Flow*, **28** No 1, pp. 31-46.
2. Huang, Y., Yang, L.J., Du, X.Z. and Yang, Y.P., 2016, Finite element analysis of thermal behaviour of metal powder during selective laser melting, *Int. J. Thermal Sciences*, **104**, pp. 146-157.
3. Foroozmehr, A., Badrossamay, M., Foroozmehr, E. and Golabi S. 2016, Finite element Simulation of Selective Laser Melting process considering Optical Penetration Depth of laser in powder bed, *Materials & Design*, **89**, No 5, pp. 255-263.
4. Gu, D., Hagedorn, Y.C., Meiners, W., Meng, G., Batista, R.J.S., Wissenbach, K. and Poprawe, R., 2012, Densification behaviour, microstructure evolution, and wear performance of selective laser melting processed commercially pure titanium, *Acta Materi.*, **60**, pp. 3849-3860.
5. Mohamad, A.A., 2011, *Lattice Boltzmann Method. Fundamentals and Engineering Applications with Computer Codes*, Springer-Verlag London Limited.
6. Krüger, T., Kusumaatmaja, H., Kuzmin, A., Shardt, O., Silva, G. and Viggen, E.M., 2017, *The Lattice Boltzmann Method. Principles and Practice*, Springer International Publishing Switzerland.
7. Krzyzanowski, M., Svyetlichnyy, D., Stevenson, G. and Rainforth, W. M., 2016, Powder bed generation in integrated modelling of additive layer manufacturing of orthopaedic implants, *Int. J. Advance Manufacturing Technology*, **87** Issue 1-4, pp. 519-530.